Monitoring therapeutic effects in experimental stroke by serial USPIO-enhanced MRI

Marilena Marinescu, Fabien Chauveau, Anne Durand, Adrien Riou, Tae-Hee Cho, Anne Dencausse, Sébastien Ballet, Norbert Nighoghossian, et al.

European Radiology

ISSN 0938-7994
Volume 23
Number 1

Eur Radiol (2012) 23:37-47
DOI 10.1007/s00330-012-2567-2

Springer

Your article is protected by copyright and all rights are held exclusively by European Society of Radiology. This e-offprint is for personal use only and shall not be self-archived in electronic repositories. If you wish to self-archive your work, please use the accepted author's version for posting to your own website or your institution's repository. You may further deposit the accepted author's version on a funder's repository at a funder's request, provided it is not made publicly available until 12 months after publication.

Springer

Author's personal copy

Eur Radiol (2013) 23:37–47
DOI 10.1007/s00330-012-2567-2

MAGNETIC RESONANCE

Monitoring therapeutic effects in experimental stroke by serial USPIO-enhanced MRI

Marilena Marinescu · Fabien Chauveau · Anne Durand · Adrien Riou · Tae-Hee Cho · Anne Dencausse · Sébastien Ballet · Norbert Nighoghossian · Yves Berthezène · Marlène Wiart

Received: 16 February 2012 / Revised: 25 May 2012 / Accepted: 2 June 2012 / Published online: 26 July 2012
© European Society of Radiology 2012

Abstract
Objectives This study sought to evaluate whether the therapeutic effects of an anti-inflammatory drug such as minocycline could be monitored by serial ultrasmall superparamagnetic particles of iron oxide (USPIO)-enhanced MRI in experimental stroke.
Methods Mice received a three-dose minocycline treatment (n=12) or vehicle (n=12) after permanent middle cerebral artery occlusion. USPIOs were administered 5 h post-surgery. MRI was performed before, 24 h and 48 h post-USPIO administration. MRI endpoints were the extent of signal abnormalities on R2 maps (=1/T2) and quantitative R2 changes over time (ΔR2). *Post-mortem* brains were prepared either for immunohistology (n=16) or for iron dosage (n=8).
Results As expected, treatment with minocycline significantly reduced infarct size, blood-brain barrier permeability and F4/80 immunostaining for microglia/macrophages. Areas of R2 maps>35 ms^{-1} also appeared significantly decreased in minocycline-treated mice (ANOVA for repeated measures, P=0.017). There was a fair correlation between these areas and the amount of iron in the brain (R^2=0.69, P=0.010), but no significant difference in ΔR2 was found between the two groups.
Conclusions This study showed that the extent of signal abnormalities on R2 maps can be used as a surrogate marker to detect minocycline effects in a murine experimental model of stroke.
Key Points
- *Ultrasmall superparamagnetic particles of iron oxide offer new avenues for MRI research*
- *Treatment of the inflammatory response following ischaemic stroke is currently undergoing evaluation.*
- *Minocycline treatment significantly reduced areas of signal abnormalities on USPIO-enhanced MRI.*
- *These areas correlated with the amount of iron in the brain.*
- *Thus USPIO-enhanced MRI might provide a surrogate marker to monitor treatment*

Keywords MRI · USPIO · Inflammation · Cerebral ischaemia · Treatment monitoring

M. Marinescu · F. Chauveau · A. Durand · A. Riou · T.-H. Cho · N. Nighoghossian · Y. Berthezène · M. Wiart (✉)
UMR CNRS 5520 CREATIS,
Hopital Louis Pradel,
Université de Lyon, Lyon 1,
28 avenue du Doyen LEPINE,
69677 Bron, France
e-mail: marlene.wiart@creatis.insa-lyon.fr

F. Chauveau · A. Durand · A. Riou · T.-H. Cho · N. Nighoghossian · Y. Berthezène
CNRS, UMR 5220; INSERM, U1044;
INSA de Lyon; Hospices Civils de Lyon;
CREATIS; Lyon,
93600 Aulnay-sous-Bois, France

A. Dencausse · S. Ballet
Guerbet Research Group,
Aulnay-sous-Bois, France

Introduction

Ischaemic stroke accounts for 88 % of all stroke cases in industrialised Western societies. To date, reperfusion therapies (thrombolysis using recombinant tissue plasminogen activator, mechanical thrombectomy catheters) are the only efficient treatments for acute stroke [1]. Considering the narrow intervention time window of up to 4.5 h after stroke onset, only a small percentage of stroke patients are in a

Author's personal copy

position to receive this therapy [2]. Stroke-induced brain damage progresses during the subacute stage up to several days after the attack, causing delayed expansion of the infarction. In addition, cerebral ischaemia triggers an inflammatory response that significantly contributes to the neurological outcome [3]. However, anti-inflammatory treatment has so far failed in clinical trials [4]. In this context, non-invasive imaging of inflammation associated with ischaemic stroke lesions could be helpful in selecting and monitoring patients who may benefit from such therapy. Magnetic resonance imaging (MRI) coupled with injection of ultrasmall superparamagnetic particles of iron oxide (USPIOs) has recently emerged as a promising tool for imaging of inflammation [5]. The USPIOs are ingested by phagocytic cells, whether within the blood pool or locally at the inflammation site. These cells thus become magnetic and detectable on MRI. USPIO-enhanced MRI has been successfully applied for pre-clinical and clinical studies of cerebral inflammation following stroke [6–8]. To the best of our knowledge, however, the ability of this technique to monitor drug effects has yet to be demonstrated.

Several anti-inflammatory strategies have been proposed to decrease ischaemic damage [9]. Minocycline is currently being evaluated in a clinical trial (Minos, Minocycline to Improve Neurologic Outcome in Stroke) [10]. Its anti-inflammatory effects were demonstrated in experimental animal stroke models: minocycline inhibited microglia/macrophage activation (part of the inflammatory response) [11, 12], protected the brain-blood barrier (BBB) [13], diminished oxidative stress [12] and infarct size [12, 14], and extended the thrombolysis therapy time window [14].

The present study sought to test the hypothesis that USPIO-enhanced MRI could monitor the therapeutic effects induced by minocycline treatment after focal cerebral ischaemia in mice.

Materials and methods

All animals were treated in strict accordance with international and institutional guidelines.

Study design

Twenty-four Swiss mice were included in the study (weight: 25 to 30 g; Charles River, l'Arbresle, France). The experimental design is detailed in Fig. 1. Briefly, on day 0 (D0), the animals underwent permanent middle cerebral artery occlusion (pMCAO, as detailed below). Minocycline (n=12) or its vehicle (n=12) was randomly administered as a three-dose intraperitoneal injection once every 3 h starting 5 min after pMCAO induction. USPIO contrast agent was administered intravenously 5 h after pMCAO. MRI was performed 4 h after pMCAO (pre-contrast), and repeated at D1 and D2 (post-contrast). Two quantitative measurements were extracted from the MRI data to compare minocycline-treated versus vehicle-treated animals: (1) USPIO brain uptake as observed on transverse relaxation rate maps (R2=1/T2) and (2) R2 change over time. The imaging protocol was followed by animal sacrifice and brain preparation for histology (n=7 in each experimental group) or iron assay (n=5 in each experimental group). All investigators either inducing stroke or assessing MRI, and post-mortem data were blinded to treatment allocation. Surgery failure, defined by the absence of lesions on pre-contrast MRI, was an exclusion criterion.

Animal model

Mice were anaesthetised with isoflurane in ambient air. Focal cerebral ischaemia was induced as described elsewhere [15, 16]. Briefly, the right MCA was exposed by subtemporal craniotomy and occluded by electrocoagulation. Wounds were then sutured and covered with lidocaine (AstraZeneca, Reims, France) to alleviate pain. During surgery, body temperature was monitored with a rectal probe and maintained at 37 °C using a feedback-regulated heating pad.

Treatment

Minocycline is a second generation antibiotic of the tetracycline family. Its half-life in rodents is approximately 2 h

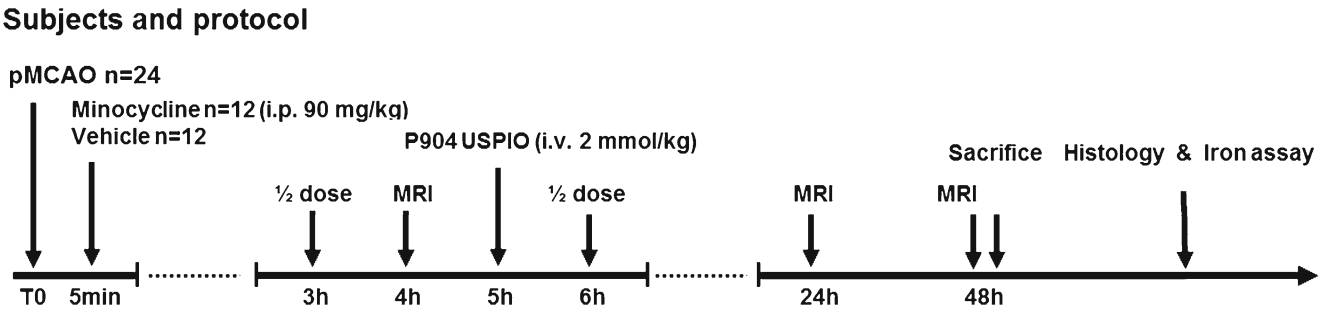

Fig. 1 Experimental design. T0 corresponds to surgery; ½ dose corresponds to 45 mg/kg minocycline administration

Author's personal copy

[17]. Minocycline (Sigma-Aldrich, Lyon, France) was dissolved in phosphate-buffered saline (PBS; 0.1 M, pH 7.4). Three injections were performed intraperitoneally at (1) 5 min (90 mg/kg), (2) 3 h (45 mg/kg), and (3) 6 h (45 mg/kg) after ischaemia [18]. Control mice received equivalent volumes (0.1 ml) of vehicle.

Contrast agent

The P904 USPIO contrast agent was provided by Guerbet Research (Aulnay-sous-Bois, France). It is composed of an 8-nm crystalline iron oxide core (maghemite γ-Fe_2O_3) coated with a hydrophilic material for stabilisation and biocompatibility. Its mean hydrodynamic diameter is 25 nm (range: 20 to 50 nm). P904 r1 relaxivity is 4 mM^{-1} s^{-1} at 4.7 T in 4 % HAS (a medium closed to plasma) at 37 °C, and r2 relaxivity is 92 mM^{-1} s^{-1} in the same conditions. A dose of 2 mmol Fe/kg body weight was injected intravenously into the tail vein 5 h post-pMCAO, i.e. 24 h before the first follow-up MRI, according to a well-documented protocol [19–21].

MRI

Experiments were performed on a 4.7-T/10-cm Bruker Biospec interfaced to a Bruker Paravision 5.0 system (Rheinstetten, Germany). A 50-mm inner-diameter birdcage coil for RF transmission and a 15-mm diameter surface coil for reception were used. The mice were placed on a bed equipped with both ear and bite holders. Body temperature was maintained at 37 ±1 °C by an integrated heating system. During image acquisition, anaesthesia was maintained using isoflurane 2 % in ambient air, and respiration was monitored with a pressure probe. The MR imaging protocol is described in Table 1. Animals were not randomised with respect to imaging time; however, they were imaged at the same time at D0, D1, and D2, thus ensuring that data were collected at the same moment post-injury for each animal (see Results).

Histology

After the last MR examination, the animals were deeply anaesthetised with isoflurane and decapitated, and the brains were dissected out. The brains were then immersed in 4 % paraformaldehyde in 100 mmol/l pH=7.4 phosphate buffer for 24 h at 4 °C, bathed for 12 h in phosphate buffer and kept in 30 % sucrose at 4 °C until use. When needed, tissues were embedded in polyethylene glycol and cut into 20-μm-thick sections by cryostat. Brain sections were hydrated in PBS and treated with 0.3 % hydrogen peroxide and methanol for 10 min to exclude any background staining by endogenous peroxidase. Microglia/macrophage detection was performed using a Histostain Plus Bulk kit (Invitrogen). Brain sections were rinsed in PBS and incubated for 10 min at room temperature with serum blocking solution (ready-to-use composition). Rat anti-mouse F4/80 antibody (clone MCA497, Serotec, Oxford, UK) diluted 1/50 in Dako S3022 solvent was applied over the brain sections for 1 h at room temperature. Sections were then rinsed three times in PBS and incubated for 20 min at room temperature with a ready-to-use biotinylated secondary antibody solution. After three rinses, the sections were treated for 10 min with enzyme conjugate followed by another cycle of PBS baths. Then 50 μl diaminobenzidine in 1 ml solvent was used to reveal the activated microglia/macrophage staining. Finally, sections were counterstained with nuclear red so as better to visualise the cytoplasm, and the iron nanoparticles were stained by Prussian blue.

For immunoglobulin deposit detection, brain sections were prepared as previously described [19]. Briefly, biotinylated sheep antimouse secondary antibody was used for brain section incubation and diaminobenzidine supplemented with

Table 1 MR imaging protocol

Imaging parameters	Spin-echo T2-weighted images	Gradient-echo (GRE) FLASH T1w	Carr-Purcell-Meiboom-Gill multi-slice multiecho (MSME)	Spin-echo diffusion-weighted images (DWI)
TE/TR (ms/ms)	75/3,500	4/157	15/4,000	28/2,000
b Values (s/mm^2)	N/A	N/A	N/A	0, 1,000
Flip angle (degrees)	180	90	180	90
No. of acquired signals	4	8	8 echoes	4
Bandwidth (kHz)	50	101	50	303
Field of view (mm^2)	20×20	20×20	20×20	30×30
Slice thickness (mm)	1	1	1	2
Number of slices	15	15	15	7
Matrix size	128×128	128×128	64×64	128×128

Note: TE = echo time; TR = repetition time; MSME sequence for R2 maps; WI = weighted imaging. DWI was performed at D0 only. Apparent diffusion coefficient (ADC) maps were generated using Paravision 5.0

Author's personal copy

nickel ammonium sulphate solution to visualise peroxidase activity.

Brain iron assay

Brain tissue was weighed, and 1 ml of cold water was added per 100 mg of tissue. Homogenisation was performed with a Gentle Macs (Myltenyi) device. The sample rested for 2 h at 4 °C to break down the foam produced by homogenisation, and then was sonicated for 30 s at 4 °C to lyse the cells completely (so as to remove the effect of compartmentalisation of the water). T1 relaxometric measurements were performed at 20 MHz and 37 °C (Minispec Bruker). The calibration curve was based on a linear regression of the form: [(1/T1−1/T1dia)]/r1=C. The product of concentration and sample weight provided the amount of iron in the brain. Product R1 in the biological matrix was previously determined by measuring the T1 of non-injected control mouse brain homogenate overloaded with increasing concentrations of P904. The T1dia (diamagnetic) value was derived from measurement in homogenates without injection.

Data analysis

All data were analysed on a personal computer (1.83 GHz, 2 Gbytes) using MIPAV software (Medical Image Processing and Visualization, NIH, Bethesda, MD, USA; http://mipav.cit.nih.gov/), as detailed below. Apart from lesion volume, all quantitative MRI and histology measurements were made on the central slice of the lesion, at the level of the corpus callosum (bregma -1.28 mm, according to Franklin and Paxinos's atlas) [22], where previous studies identified specific USPIO-related changes over time [19, 21].

MRI analysis

T2-weighted images revealed a sharp transition between the lesion and healthy tissue at baseline and even after USPIOs injection (see Fig. 3, T2-WI, D1 and D2). Therefore, lesions were manually outlined on T2-weighted images at all timepoints. Volumes were calculated by summation of the lesion areas of all brain slices showing brain damage and integration by slice thickness. Brain swelling (increased ipsilateral hemisphere volume compared with contralateral) was assessed by dividing the ipsilateral (IH) by the contralateral hemisphere (CH) value: IH/CH. To avoid overestimation attributable to brain swelling, lesion volume (V) was normalised by the ratio: VxCH/IH.

Transverse relaxation rate maps (R2=1/T2) were generated from MSME native images using MRIUtil software (Penn State Hershey, Hershey, PA, USA; http://www.pennstatehershey.org/web/nmrlab/resources/software/mriutil).

The USPIO brain uptake induces hypointense signals on post-contrast T2-weighted images, reflecting higher R2 relaxation rates, which translate on R2 maps into hyperintense signals. Extent of USPIO uptake was defined automatically by thresholding R2 maps so as to encompass the hyperintense zone corresponding to USPIO accumulation areas (Fig. 2a). A threshold of 35 s^{-1} was applied, based on in vitro calibration curves [23].

Quantitative R2 measurements were made using a four-pixel (0.39 mm^2) region of interest (ROI) placed on the R2 maps, in systematically identical locations at D0, D1, and D2: (1) in contralateral healthy tissue, (2) lesion core, (3) lesion periphery, and (4) the contralateral corpus callosum. The contralateral healthy tissue R2 values were used to normalise those obtained in the other three ROIs. Changes in R2 over time were calculated as: ΔR2(Di)=R2(Di)-R2(D0), with i=1 and 2.

Histology analysis

Extents of F4/80+ cells and BBB permeability to IgG were measured by manually outlining areas of positive staining on respective slices (Fig. 2b and Fig 2c). The mean number of F4/80+ round-shaped cells was made by averaging cell counts performed on three consecutive slices using a 0.06 mm^2 region of interest placed systematically in the same area in the periphery of the lesion.

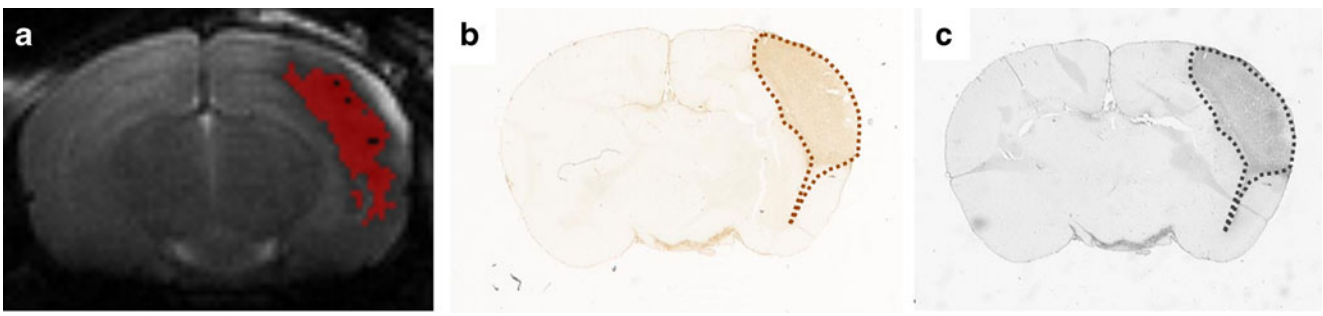

Fig. 2 (**a**) Extent of USPIO uptake automatically defined by thresholding R2 maps. (**b**) Extent of F4/80+ cells and (**c**) extent of BBB permeability to IgG as defined by manually outlining areas of positive staining

Author's personal copy

Statistical analysis

Statistical analysis was performed with the SPSS 11 statistical software package for Windows (SPSS, Chicago, IL, USA). Data are given as mean values ± standard deviation, and presented as scatter plots showing individual values. MRI data were evaluated statistically by analysis of variance for repeated measures using the general linear model. Additional intra-group comparison (D1 vs. D2) was performed using the Wilcoxon signed-rank test. Non-parametric Mann-Whitney tests were used for inter-group comparison of post-mortem measurements. Spearman correlation coefficients (r_s) were computed to assess the relationship between the extent of USPIO uptake and iron dose, lesion size, F4/80+ and IgG + areas. *P* values less than 0.05 were considered significant for all statistical analyses.

Results

All animals survived the protocol. Three mice were excluded because of surgery failure (1 in the vehicle group and 2 in the minocycline group). In all other animals, surgery resulted in a reproducible focal lesion in the cortex and the dorsal part of the striatum [Fig. 3, apparent diffusion coefficient (ADC), arrowhead].

MRI

T2-WI obtained at D1 (23 h±2 h) and D2 (47 h±2 h) after USPIO administration showed areas of signal loss in the perilesional area, around CSF compartments (ventricles and velum), and along the ipsilateral corpus callosum, in all mice in both the vehicle and minocycline-treated groups (Fig. 3, T2-WI). In half of the animals (7/11 in the vehicle group and 5/10 in the minocycline-treated group), the regions of signal loss extended into the contralateral part of the corpus callosum. Acute transcallosal deafferentation might be responsible for this phenomenon [21]. The hypointense signal seen on T2-WI was observed as a hyperintense signal on gradient echo (GRE) T1-weighted images at D1, which shifted to a hypointense signal at D2 (Fig. 3, GRE, arrows). These observations were in line with those of previous studies studying non-treated animals [19, 21].

Figure 4 presents lesion volumes and brain swelling, repeatedly measured on D0, D1, and D2, in both groups. Lesion sizes were significantly smaller in minocycline-treated mice than in control mice (P=0.006) (Fig. 3a). Brain swelling was also significantly reduced in minocycline-treated compared with control mice (P=0.003) (Fig. 4b).

The USPIO uptake was significantly affected by time and treatment: thresholded areas were lower on D2 than on D1 (P=0.04), and were decreased by minocycline treatment (D1, vehicle: 9±4 mm^2 vs. minocycline: 6±3 mm^2; D2, vehicle: 7±2 mm^2 vs. minocycline: 4±3 mm^2; P=0.017) (Fig. 5a). There was no correlation between the extent of USPIO uptake (as measured by areas with R2>35 ms^{-1}) and lesion size at any timepoint.

Pre-contrast R2 values in healthy tissue and ΔR2 values are shown in Table 2. R2 values in healthy tissue did not significantly vary over time, indicating that USPIOs had been washed out of the circulating blood by D1. No significant difference between the two groups was found at any of the time points in the lesion (P=0.68) or in the corpus callosum (P=0.175). Perilesional measurements tended to show a treatment effect (P=0.063), in addition to a significant time effect (P=0.005). Indeed, ΔR2 values at D2 were significantly decreased compared with D1 values in the vehicle-treated group (P=0.016), but not in the minocycline group (P=0.386).

Histology

F4/80-positive cells with the round morphological features of phagocytic cells were detected in the lesion, at the periphery of the lesion, around the CSF compartments (ventricles and velum) and in the corpus callosum, for both vehicle and treated groups (Fig. 6a), in co-localisation with areas of signal loss on T2-WI (Fig. 2 and Fig. 3). Double staining with Prussian blue and F4/80 suggested that iron particles were internalised by macrophages (Fig. 6a2 and a3). IgG immunostaining was found in the lesion, the perilesional area, around the CSF compartments, and in the ipsilateral corpus callosum, in both groups (Fig. 6b).

Again, these findings reproduced the results of a previous study using the same animal model [19].

The necrotic part of the lesion tended to fall apart during brain dissection, making quantitative damage assessment difficult. One brain in the vehicle group could not be analysed, and six animals were finally included in each group. Despite this limitation, areas of F4/80+ cells were found to be significantly smaller in the minocycline-treated group (6±1 mm^2) than in the vehicle-treated group (13±2 mm^2; P=0.020) (Fig. 5c). There was also a significant difference in the IgG-positive area between the two groups (vehicle: 11±4 mm^2 vs. minocycline-treated: 6±1 mm^2; P=0.020) (Fig. 5c). In the perilesional area, there were fewer F4/80+ round-shaped cells in the minocycline-treated group; however, the difference was not statistically significant (vehicle: 42±8 vs. minocycline-treated: 34±19; P=0.34) (Fig. 5d).

Correlations between the extent of USPIO uptake at D2 (as measured by areas with R2>35 ms^{-1}) and F4/80+ and IgG + areas appeared not significant (r_s=0.48, P=0.118 and r_s=0.54, P=0.071 respectively). However, when two outliers were excluded from the analysis (one in the minocycline

Author's personal copy

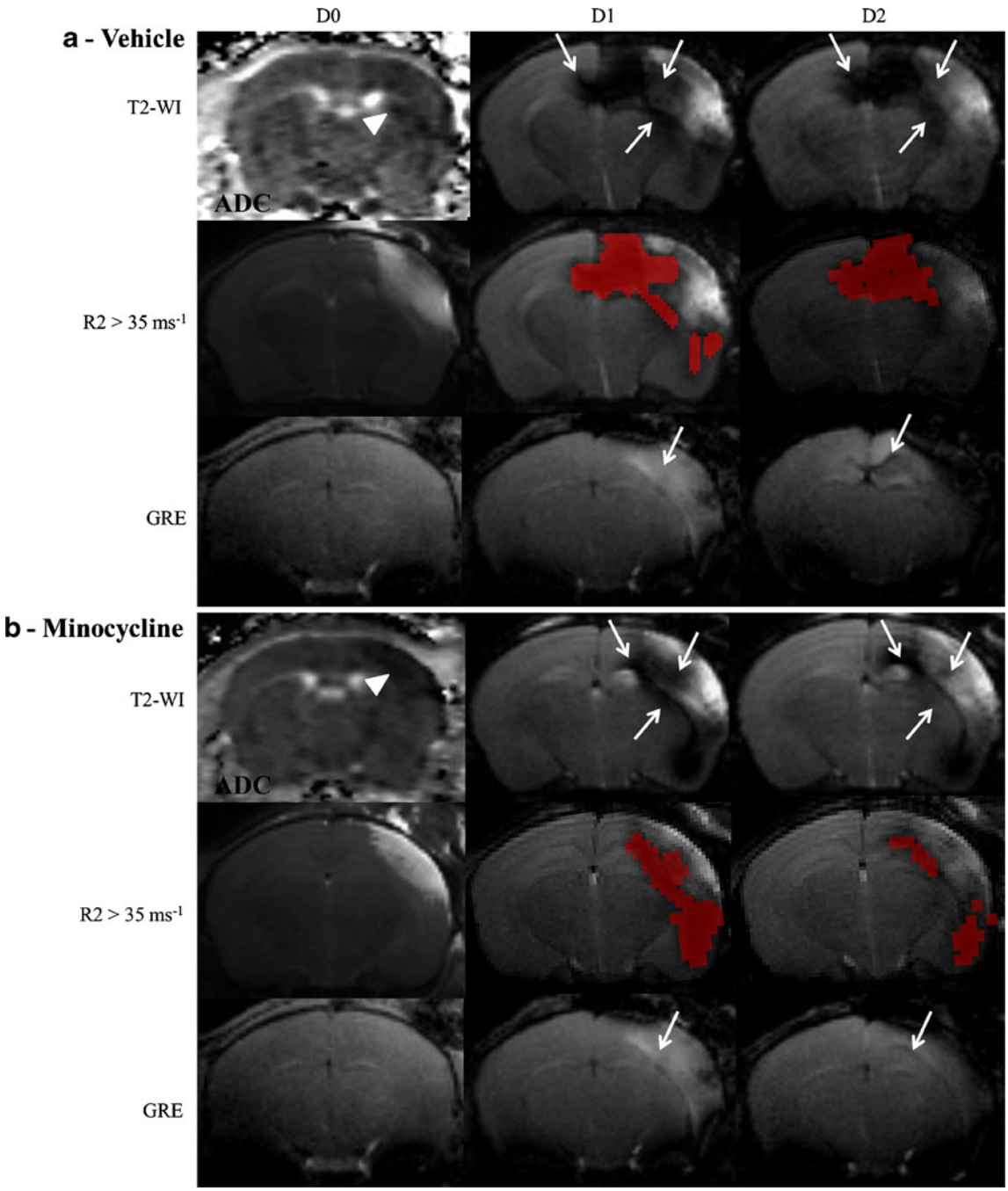

Fig. 3 USPIO distribution over 2 days in a transverse slice through mouse brain (bregma -1.28, according to Franklin and Paxinos's atlas) observed on multiparametric MRI in a vehicle-treated (**a**) and a minocycline-treated mouse (**b**). D0 corresponds to pre-contrast and D1 and D2 to post-contrast data. T2-WI: Note the larger lesion size in the vehicle-treated animal compared with the minocycline-treated animal at D0 (shown as hypointense signal on ADC maps) and the marked T2 signal decrease induced by USPIOs in the lesion, the perilesional area, and in the corpus callosum at D1 and D2 (arrows). R2>35 ms^{-1}: Red voxels represent the result of automatic segmentation by thresholding R2 maps. Note how segmented areas visually corresponded to areas of hypointense signals on T2-WI. GRE: Note the transition from hyperintense (D1) to hypointense (D2) signal (arrows), most likely related to USPIO's internalisation. T2-WI: T2-weighted imaging; GRE: gradient echo imaging

group and one in the vehicle group: Fig. 5, red circles), good and statistically significant correlations were highlighted between the extent of USPIO uptake at D2 and both F4/80+ (Fig. 5e, r_s=0.82, P=0.004) and IgG+(Fig. 5f, r_s=0.86, P=0.002) areas. The outliers corresponded to animals with average lesion size compared to their respective groups, but showing particularly marked signal loss following USPIO administration.

Author's personal copy

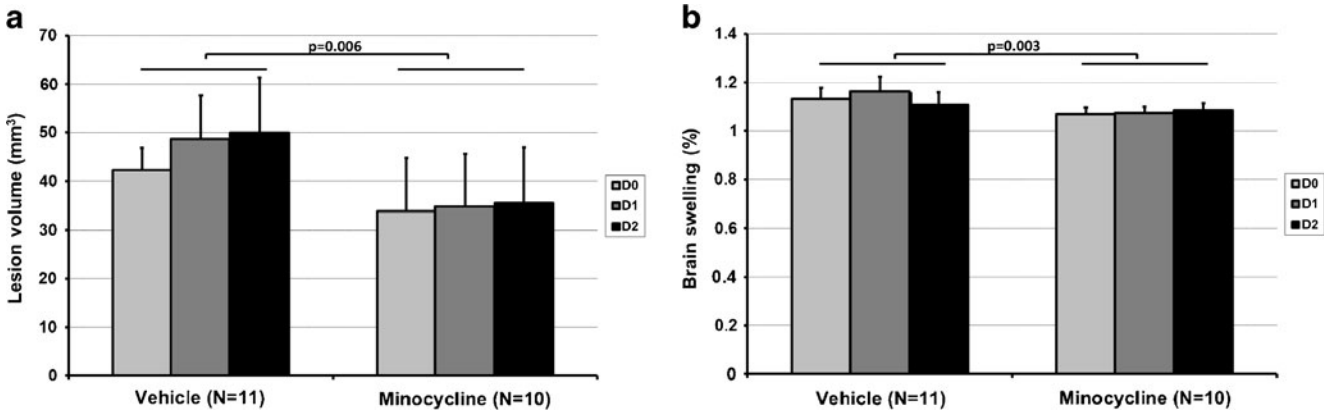

Fig. 4 Evolution in time of lesion volumes (after correction for brain swelling) (**a**) and brain swelling (**b**) in vehicle-treated (N=11) and minocycline-treated (N=10) groups

Brain iron assay

On relaxometric assay, iron uptake in brain tissue was 11± 4 nmol in the control group (n=4) and 5±2 nmol in the minocycline-treated group (n=4); this difference did not reach significance (P=0.20). On the other hand, there was a good correlation between the iron assay results and USPIO uptake measured at D2 (Fig. 5b, r_s=0.83, P=0.010).

Discussion

Post-stroke inflammation is a therapeutic target of considerable interest because its therapeutic window is potentially wider than that offered by thrombolysis. Imaging surrogate markers are urgently needed to monitor such therapy so as to finely tune the complex inflammatory cascade. Inflammation imaging currently relies on macrophage detection. This can be achieved by PET, using PBR/TSPO radioligands, or by MRI, using iron oxide nanoparticles. As MRI is increasingly used for the management and selection of stroke patients for thrombolysis, surrogate MRI outcome measures are becoming an important component of translational research. We show here, to our knowledge for the first time, that MRI enhanced with USPIO enables monitoring of anti-inflammatory treatment.

Several studies suggested that minocycline treatment could inhibit ischaemia-induced activation of microglia through post-mortem immunohistochemical staining [11, 13–24]. Recently, Martin et al. measured a significant decrease in macrophage-specific radiotracer uptake after minocycline treatment in a rat model of transient focal cerebral ischaemia [25]. In their study, however, PET data were not validated against immunohistochemistry. The present study combined (1) in vivo imaging by USPIO-enhanced MRI, (2) post-mortem measurement of brain contrast-agent uptake on relaxometry, and (3) post-mortem detection of both contrast agent and one of its cellular targets on immunohistochemistry. As expected, minocycline treatment induced a decrease in: (1) lesion size, (2) BBB permeability to IgG, and (3) F4/80 immunostaining for macrophage/microglia.

A significant difference in lesion size was observed at the earliest time point (D0). Although this early time point (4 h post-occlusion) was not evaluated in previous studies, this result was not expected, as anti-inflammatory mechanisms are considered to occur later at the acute stage. Alternatively, antioxidant mechanisms involved in the very first hours after cerebral ischaemia [12] may explain a difference in lesion initiation between minocycline-treated mice and controls. MRI could not be performed before treatment initiation to check if distribution of initial lesion sizes was similar in each group because delayed minocycline administration shows no significant benefit after insult, unlike early administration [12]. To minimise this bias, allocation was randomised and concealed to the investigator responsible for stroke induction, according to STAIR recommendations for preclinical trials [26]. Lesion size was not the primary endpoint of the current work, in which minocycline was chosen because it represented a drug with both anti-inflammatory properties and clinical relevance [27].

In this specific model of pMCAO, USPIO enhancement at 24 h post-injury has been shown to be mainly caused by non-specific mechanisms such as BBB leakage, rather than by peripheral phagocyte infiltration [19]. At 48 h, most iron-related signal changes on MRI are indisputably paralleled by phagocyte-associated iron deposition detected on histology [21]. These phagocytic cells are usually thought to be macrophages [5], although it remains unclear which subtype is labelled, and in which proportion. Again, these questions were not primarily addressed in the present work, which confirmed the basic findings of previous studies showing that F4/80+ cells had phagocytosed USPIOs at D2 post-injury [21].

Author's personal copy

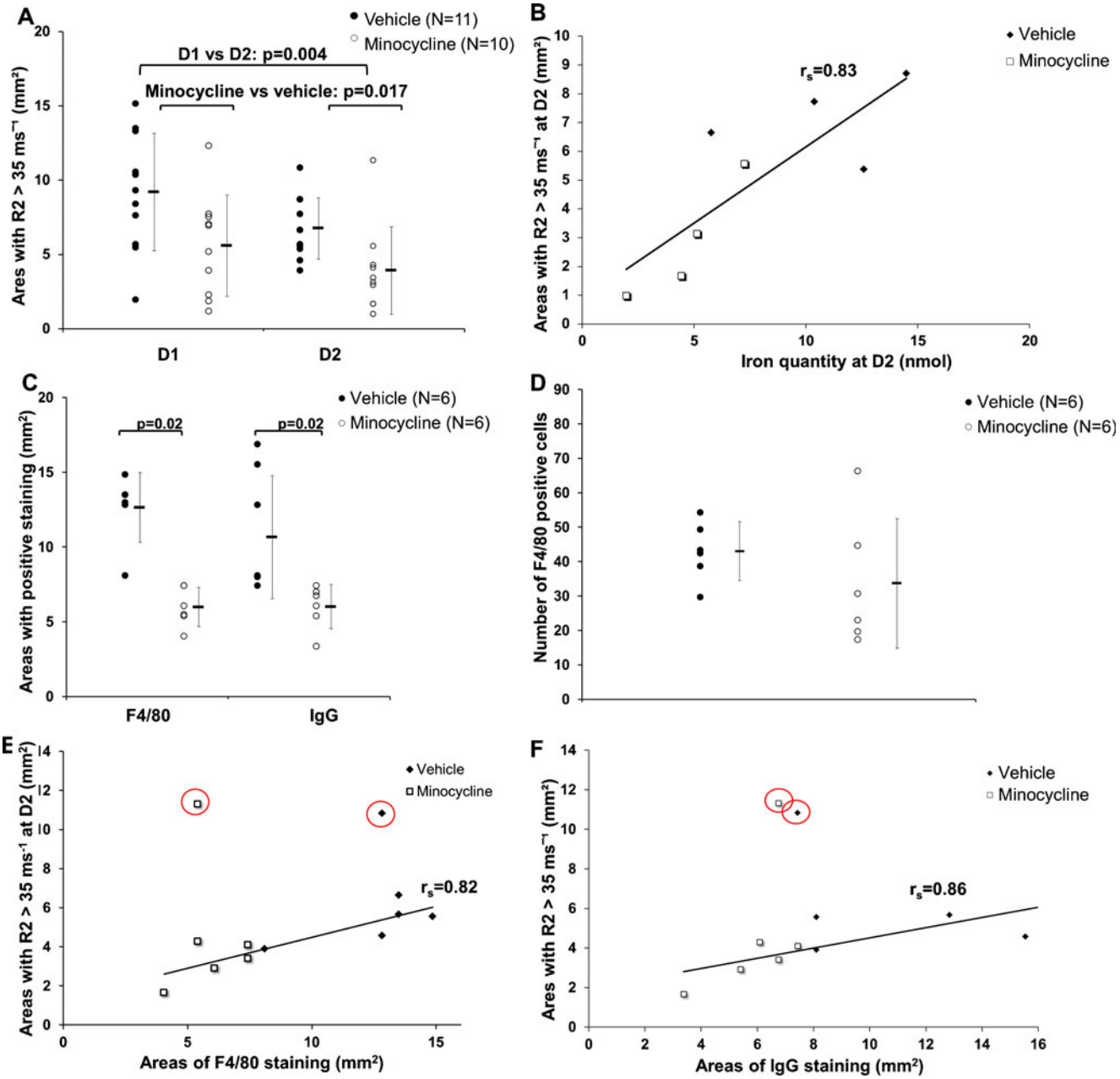

Fig. 5 MRI, immunohistological, and iron assay endpoints. (**a**) Areas of USPIO uptake quantified from thresholding R2 maps at D1 and D2. (**b**) Correlation between post-mortem relaxometric iron dosage and R2 maps thresholded areas at D2. (**c**) Areas of F4/80 and IgG staining measured from histological slices at D2. (**d**) F4/80+ round-shaped cells count at D2. (**e**) Correlation between R2 map thresholded areas and F4/80+ areas. (**f**) Correlation between R2 maps thresholded areas and IgG + areas. Spearman correlation coefficients (r_s) are given after excluding outliers (circled in red)

Despite these unsolved issues concerning the mechanism of action of minocycline, and of the USPIO mechanism of labelling, we present here a proof-of-concept study validating USPIO uptake as an imaging index sensitive to treatment. However, to date, a major limitation of the technique is clearly the inability to unequivocally discriminate between multiple drug effects on BBB breakdown and on phagocytic activity. Indeed, it could very well be that the extent of USPIO uptake mainly reflected contrast agent leakage into the brain. USPIO ingestion by phagocytic cells might then appear reduced in the minocycline group only because of reduced availability in the brain. Assessment of BBB disruption at the time of USPIO injection using a gadolinium chelate was not performed in the current work because it is technically challenging to perform two consecutive intravenous injections in the same mouse; however T1 enhancement of the entire lesion has been reproductively showed after gadolinium chelate injection at 6 h post-

Author's personal copy

Table 2 R2 (in healthy tissue) and ΔR2 measurements in s^{-1} given as mean ± standard deviation

Measure	R2			ΔR2					
Locus	Contralateral healthy tissue			Lesion		Perilesional area		Corpus callosum	
Time point	D0	D1	D2	D1	D2	D1	D2	D1	D2
Vehicle (n=11)	22±2	21±1	20±1	17±15	12±11	13±8	5±3*	18±17	13±9
Minocycline (n=10)	19±2	20±1	20±1	13±14	12±15	7±3	5±5	9±14	8±12

*D2 vs. D1, Wilcoxon signed-rank test: P=0.016

pMCAO [19, 21]. To test the hypothesis of reduced availability of USPIOs, one would then need to quantify the amount of free USPIO in the brain at D1. However, this could not be done using histological approaches because of the well-known lack of sensitivity of Prussian blue to interstitial USPIO (as opposed to iron compartmentalised in cells) [19, 28, 29], or using iron dosages as these do not discriminate between free and compartmentalised USPIOs. Even techniques such as electronic microscopy would only provide a visual assessment of the presence of free USPIOs, not, to the best of our knowledge, a quantitative one.

Conversely, what are the arguments in favour of MRI monitoring of phagocytosis inhibition? USPIO cell internalisation induces a decrease in T2 relaxivity [30]. This effect could explain in part the significant decrease in the extent of USPIO uptake between D1 and D2 observed in both groups,

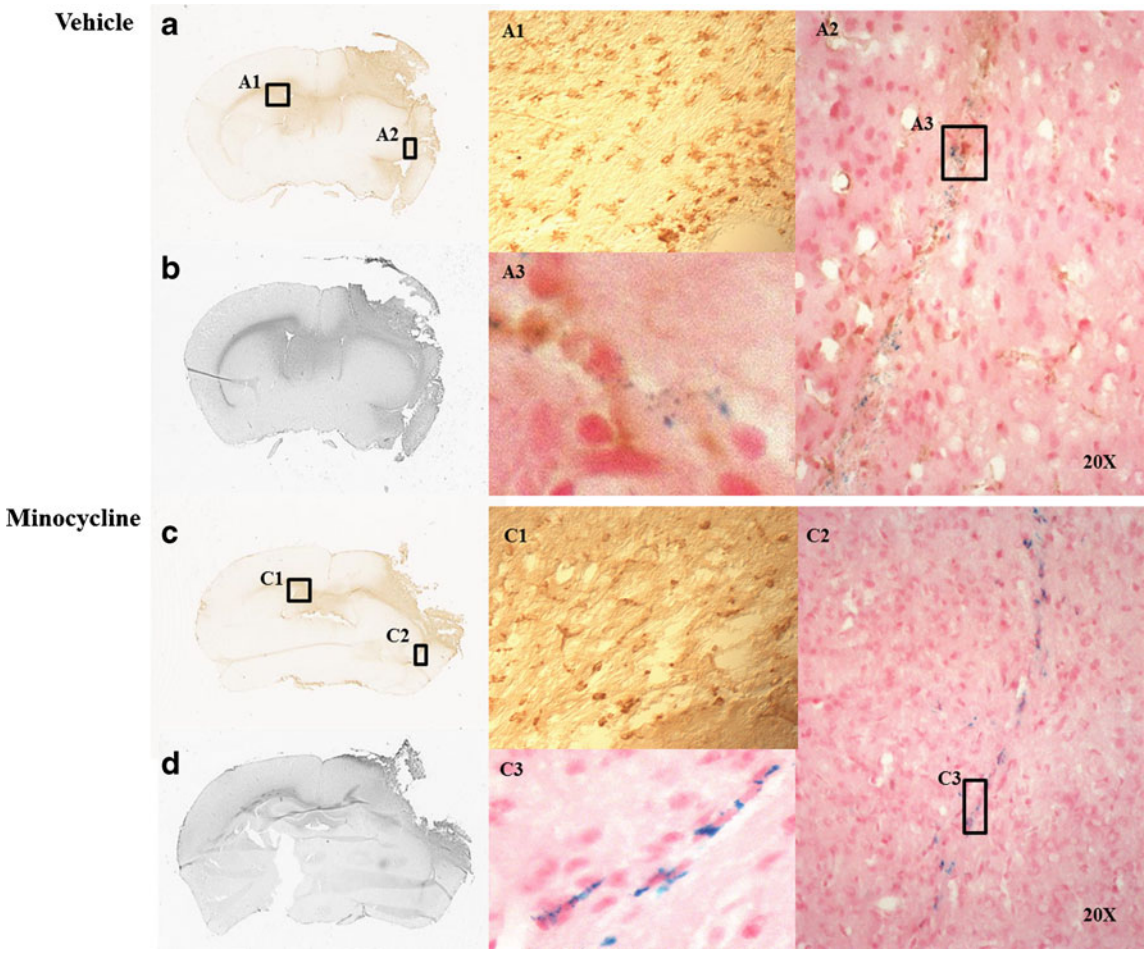

Fig. 6 Representative snapshots of immunohistology in a vehicle-treated mouse (**a** and **b**) and a minocycline-treated mouse (**c** and **d**). Positive staining can be seen in the lesion, perilesional area, corpus callosum, and around the ventricles with F4/80 immunostaining for microglia/macrophages (**a** and **c**) and IgG as a marker of BBB disruption (**b** and **d**). Magnification of a region in the corpus callosum shows brown F4/80+ reactive cells (**a**1, **c**1). Prussian blue and F4/80 double staining shows multiple Prussian blue+ spots associated with F4/80+ cells (**a**2, **c**2). Prussian blue staining around the nucleus suggests USPIO cell internalisation (**a**3, **c**3)

Author's personal copy

as in some regions, R2 would then fall below the threshold (see thereafter for discussion of this limitation). The decrease in USPIO uptake extent at D2 might also be influenced by migrating and gathering of iron-labelled cells in chemoattracting regions, such as the lesional and/or perilesional area (as seen in Fig. 5 for instance). Interestingly, there was a statistically significant reduction in ΔR2 from D1 to D2 in the perilesional area of the vehicle group, while ΔR2 remained constant in the minocycline-treated group. These findings suggested enhanced local phagocytic activity in the non-treated group [30]. The trend towards lower round-shaped cells in the perilesional area of minocycline-treated mice provided an argument in favour of this interpretation, although studies involving more animals are warranted to confirm this result.

One limitation of the segmentation approach is that the result is dependent on the choice of threshold. It is therefore mandatory to apply the technique to maps generated from reproducible quantities such as R2. Both phantom and animal studies showed a linear relationship between R2 and USPIO concentration [30, 31], so that the threshold can be taken as reflecting a given amount of iron oxide. The healthy mouse brain presents homogeneous pre-contrast R2 values (around 20 ms^{-1} at 4.7 T) that do not substantially vary from one region to another. However, vasogenic oedema in the ischaemic lesion induces a drop in pre-contrast R2 (around 8 ms^{-1} at 4.7 T). As a consequence, a single threshold for post-contrast R2 may in fact reflect a range of iron concentrations [(1.2–2.4) mmol Fe/ml for free iron, and 30 % less for internalised iron]. We therefore checked: (1) that thresholding resulted in areas visually corresponding to hypointense signals on T2-WI and (2) that the resultant extent of USPIO uptake was linearly related to the amount of iron in the brain, as measured post-mortem on T1 relaxometry. Although the additional positive correlations between the extent of USPIO uptake and F4/80+ and IgG+ areas are encouraging, there are obvious limitations in comparing areas from two methods without co-registering the images in order to evaluate the actual match between the two. However, co-registration of histology with MR images is difficult, because of the disparity in scale (in-plane resolution and slice thickness) as well as tissue distortion that occurs when live tissue is fixed and sectioned.

Another drawback of the thresholding approach is represented by a potential loss of sensitivity for internalised cells in regions with a low density of phagocytic cells. In most cases, areas of R2 hyperintense signals were smaller than areas covered by F4/80+ cells and IgG + staining (Fig. 2 and 5), despite the blurring and partial volume effects of MR images. This may be explained by the fact that manual contouring of histological slices encompassed regions of weak (e.g. lesion core) as well as high density (e.g., perilesional area), whereas automatic segmentation specifically highlighted high spots.

In summary, as minocycline has a broad spectrum of interdependent therapeutic effects, it should be acknowledged that both a decrease in BBB permeability and inhibition of phagocytosis may have influenced the USPIO-enhanced MRI findings. Despite this limitation, one might argue that because future strategies for stroke treatment involve a combination of therapies [32], a functional imaging technique providing synthesised information about two of the multiple mechanisms of action might still prove useful in a translational prospect. For example BBB protection by minocycline could reduce damage associated with reperfusion, hence the association with thrombolysis in the Minos study [10]. Although there are still several limitations to overcome before the widespread application of the technique in clinical practice (such as elucidating the USPIO entrance route into the brain of stroke patients or defining R2 thresholds in the more complex human brain), USPIO-enhanced MRI might provide useful surrogate markers for detecting a therapeutic effect in pre-clinical studies.

Acknowledgements This work was supported by a grant from the ANR TecSan (INFLAM). We would like to thank Jean-Christophe Brisset (Department of Radiation Oncology, University of Michigan, Ann Arbor, MI 48109, USA) for performing preliminary work for this study. We also thank Serge Nataf, Marie Chanal and Chantal Watrin from INSERM U842, Laennec School of Medicine, University of Lyon for helping with the histology analysis. We are grateful to Mehrnaz Jafarian-Tehrani from the EA4475 Pharmacology Laboratory (Paris Descartes University) for providing us with the minocycline treatment protocol.

Conflict of interest Anne Dencausse, employee of Guerbet Group. Sebastien Ballet, employee of Guerbet Group.

References

1. Adams HP Jr, del Zoppo G, Alberts MJ et al (2007) Guidelines for the early management of adults with ischemic stroke: a guideline from the American Heart Association/American Stroke Association Stroke Council, Clinical Cardiology Council, Cardiovascular Radiology and Intervention Council, and the Atherosclerotic Peripheral Vascular Disease and Quality of Care Outcomes in Research Interdisciplinary Working Groups: the American Academy of Neurology affirms the value of this guideline as an educational tool for neurologists. Stroke 38:1655–1711
2. Hacke W, Kaste M, Bluhmki E et al (2008) Thrombolysis with alteplase 3 to 4.5 hours after acute ischemic stroke. N Engl J Med 359:1317–1329
3. Danton GH, Dietrich WD (2003) Inflammatory mechanisms after ischemia and stroke. J Neuropathol Exp Neurol 62:127–136
4. Durukan A, Tatlisumak T (2007) Acute ischemic stroke: overview of major experimental rodent models, pathophysiology, and therapy of focal cerebral ischemia. Pharmacol Biochem Behav 87:179–197
5. Corot C, Petry KG, Trivedi R et al (2004) Macrophage imaging in central nervous system and in carotid atherosclerotic plaque using ultrasmall superparamagnetic iron oxide in magnetic resonance imaging. Invest Radiol 39:619–625

Author's personal copy

6. Chauveau F, Cho TH, Berthezene Y, Nighoghossian N, Wiart M (2011) Imaging inflammation in stroke using magnetic resonance imaging. Int J Clin Pharmacol Ther 48:718–728
7. Nighoghossian N, Wiart M, Cakmak S et al (2007) Inflammatory response after ischemic stroke: a USPIO-enhanced MRI study in patients. Stroke 38:303–307
8. Bernd H, De Kerviler E, Gaillard S, Bonnemain B (2009) Safety and tolerability of ultrasmall superparamagnetic iron oxide contrast agent: comprehensive analysis of a clinical development program. Invest Radiol 44:336–342
9. Emsley HC, Tyrrell PJ (2002) Inflammation and infection in clinical stroke. J Cereb Blood Flow Metab 22(12):1399–1419
10. Planas AM, Traystman RJ (2010) Advances in translational medicine. Stroke 42:283–284
11. Yrjanheikki J, Tikka T, Keinanen R, Goldsteins G, Chan PH, Koistinaho J (1999) A tetracycline derivative, minocycline, reduces inflammation and protects against focal cerebral ischemia with a wide therapeutic window. Proc Natl Acad Sci U S A 96:13496–13500
12. Morimoto N, Shimazawa M, Yamashima T, Nagai H, Hara H (2005) Minocycline inhibits oxidative stress and decreases in vitro and in vivo ischemic neuronal damage. Brain Res 1044:8–15
13. Machado LS, Sazonova IY, Kozak A et al (2009) Minocycline and tissue-type plasminogen activator for stroke: assessment of interaction potential. Stroke 40:3028–3033
14. Murata Y, Rosell A, Scannevin RH, Rhodes KJ, Wang X, Lo EH (2008) Extension of the thrombolytic time window with minocycline in experimental stroke. Stroke 39:3372–3377
15. Chauveau F, Moucharrafie S, Wiart M et al (2011) In vivo MRI assessment of permanent middle cerebral artery occlusion by electrocoagulation: pitfalls of procedure. Exp Transl Stroke Med 2:4
16. Pialat JB, Cho TH, Beuf O et al (2007) MRI monitoring of focal cerebral ischemia in peroxisome proliferator-activated receptor (PPAR)-deficient mice. NMR Biomed 20:335–342
17. Andes D, Craig WA (2002) Animal model pharmacokinetics and pharmacodynamics: a critical review. Int J Antimicrob Agents 19:261–268
18. Homsi S, Federico F, Croci N et al (2009) Minocycline effects on cerebral edema: relations with inflammatory and oxidative stress markers following traumatic brain injury in mice. Brain Res 1291:122–132
19. Desestret V, Brisset JC, Moucharrafie S et al (2009) Early-stage investigations of ultrasmall superparamagnetic iron oxide-induced signal change after permanent middle cerebral artery occlusion in mice. Stroke 40:1834–1841
20. Rausch M, Sauter A, Frohlich J, Neubacher U, Radu EW, Rudin M (2001) Dynamic patterns of USPIO enhancement can be observed in macrophages after ischemic brain damage. Magn Reson Med 46:1018–1022
21. Wiart M, Davoust N, Pialat JB et al (2007) MRI monitoring of neuroinflammation in mouse focal ischemia. Stroke 38:131–137
22. Franklin (1997) The Mouse Brain In Stereotaxic Coordinates(ed)^(eds) San Diego, Calif:Academic Press
23. Brisset JC, Sigovan M, Chauveau F et al (2011) Quantification of iron-labeled cells with positive contrast in mouse brains. Mol Imaging Biol 13:672–678
24. Yenari MA, Xu L, Tang XN, Qiao Y, Giffard RG (2006) Microglia potentiate damage to blood-brain barrier constituents: improvement by minocycline in vivo and in vitro. Stroke 37:1087–1093
25. Martin A, Boisgard R, Kassiou M, Dolle F, Tavitian B (2010) Reduced PBR/TSPO expression after minocycline treatment in a rat model of focal cerebral ischemia: a PET study using [(18)F] DPA-714. Mol Imaging Biol
26. Fisher M, Feuerstein G, Howells DW et al (2009) Update of the stroke therapy academic industry roundtable preclinical recommendations. Stroke 40:2244–2250
27. Fagan SC, Waller JL, Nichols FT et al (2010) Minocycline to improve neurologic outcome in stroke (MINOS): a dose-finding study. Stroke 41:2283–2287
28. Rausch M, Baumann D, Neubacher U, Rudin M (2002) In-vivo visualization of phagocytotic cells in rat brains after transient ischemia by USPIO. NMR Biomed 15:278–283
29. Stroh A, Zimmer C, Werner N et al (2006) Tracking of systemically administered mononuclear cells in the ischemic brain by high-field magnetic resonance imaging. NeuroImage 33:886–897
30. Brisset JC, Desestret V, Marcellino S et al (2009) Quantitative effects of cell internalization of two types of ultrasmall superparamagnetic iron oxide nanoparticles at 4.7 T and 7 T. Eur Radiol 20:275–285
31. Sigovan M, Boussel L, Sulaiman A, et al. (2009) Rapid-clearance iron nanoparticles for inflammation imaging of atherosclerotic plaque: initial experience in animal model. Radiology 252:401-409
32. Fisher M, Davalos A, Rogalewski A, Schneider A, Ringelstein EB, Schabitz WR (2006) Toward a multimodal neuroprotective treatment of stroke. Stroke 37:1129–1136